Phase Separation and Hydrothermal Degradation of 3 mol Y₂O₃ ZrO₂ Ceramics.

Isao YAMASHITA

Koji TSUKUMA

Phase separation and hydrothermal degradation of 3 mol% Y_2O_3 stabilized tetragonal ZrO_2 polycrystal (3Y TZP) have been studied by means of x ray diffractometry. The Rietveld analysis revealed that the crystal structure of the sintered body remarkably changes at high temperatures. The sintered body underwent phase separation into high and low yttrium regions with increasing sintering temperatures. The tetragonal phase was assigned to both regions. The high yttrium region was analyzed on the basis of a tetragonal phase model of c/a 1. The amount of monoclinic phase induced by hydrothermal degradation increased with the increase of degradation time. The aging kinetics of the tetragonal to monoclinic phase transition was analyzed using Johnson Mehl Avrami equation. The fraction of a transformable phase evaluated by the equation was in good agreement with the fraction of low yttrium region derived from the Rietveld analysis. Quantitative analysis showed that the low yttrium region selectively transforms into monoclinic phase under the hydrothermal condition, while the high yttrium region remains unchanged. The fraction of 3Y TZP ceramics transformable under hydrothermal condition was governed by the amount of low yttrium region. Thus, the formation of low yttrium region due to phase separation is responsible for the hydrothermal degradation of the sintered bodies.

Introduction

Numerous studies have been made on Y_2O_3 stabilized tetragonal ZrO_2 polycrystal (Y-TZP) in the past decades. Especially, 3 mol Y_2O_3 doped systems (3Y-TZP) have been studied extensively because of its high toughness and strength [1]. The tetragonal structure in sintered body is closely related to the mechanical property, because the enhanced toughness and strength are attributed to the stress-induced phase transition of tetragonal phase [2].

The tetragonal to monoclinic phase transition is accelerated under hydrothermal conditions. This phenomenon is called the hydrothermal degradation of tetragonal zirconia. Although many attempts have been made to explain the hydrothermal degradation, the mechanism is still controversial. So far, two major theories have been proposed to explain the degradation mechanism. One is the drawing out of yttrium from Y

TZP by means of either the formation of such compound as $Y(OH)_3$ [3] or the direct leaching [4]. The other is the termination of Zr O Zr bonds near the surface by attack of H_2O molecules. Sato *et al.* [5] reported that the termination of Zr O Zr bonds leads to the reduction of strain near the surface. The reduction of lattice strain reduces the Gibbs free energy gap between the tetragonal and monoclinic phases. Yoshimura *et al.* [6] suggested that the termination of Zr O Zr bonds allows OH ion to penetrate into the tetragonal lattice and consequently to reduce an energy barrier of nucleation for the tetragonal to monoclinic phase transition.

Although the tetragonal to monoclinic phase transition (so called martensitic phase transition) plays an important role not only for the high toughness mechanism but also for the hydrothermal degradation mechanism, only few studies have so far been made on the crystal structure of the sintered body.

Recently, the heterogeneity caused by yttrium segregation and cubic formation has been reported for 3Y TZP ceramics using high resolution TEM [7-10]. Matsui et al. [8-10] reported that the enrichment of yttrium exclusively occurs along the grain boundary and the solute dragging effect of yttrium plays an important role for the grain-growth mechanism.

In this study, the structural changes of the sintered body were analyzed using the Rietveld analysis as a function of sintering temperature. The aging kinetics of the tetragonal to monoclinic phase transition was also analyzed with an equation for nucleation-growth mechanism. The correlation between the phase separated state of the sintered body and the hydrothermal degradation phenomena have been discussed.

Experimental

Commercially available 3Y TZP powder of a specific surface area 16 m^2/g (TZ 3Y grade, Tosoh, Tokyo, Japan) was used as the starting material. The powder was synthesized by the hydrolysis method. The 3Y TZP powder was pressed uniaxially into a disk at 70 MPa and then isostatically cold pressed at 200 MPa. The green compacts were sintered at 1100, 1200, 1300, 1400 and 1500 in air for 2 h with a constant heating rate of 100 /h. The bulk density of the sintered bodies was measured by the Archimedes method. The hydrothermal degradation experiments were carried out on the samples sintered at 1500 at 140 using a pressure-resistant stainless vessel for a period of 3 to 48 h.

The x ray diffractometry was made at room temperature using a powder diffractometer system (Model MXP, MAC Science Co. Ltd., Tokyo, Japan) with the Cu Ka radiation source, under 40 KV and 30 mA. The diffraction data were collected in the area 2 = 20 to 90 ° with a step of 0.04 °. Intensity was integrated for 20 sec at each step. Measurements were made on an as-sintered surface of the sintered body.

The diffraction data were analyzed by the Rietveld method with a program Rietan 2000 [11], where the structural parameters reported by Yashima et al. [12], Morinaga et al. [13], and Howard et al. [14] were used as the initial parameters for the tetragonal, cubic and

monoclinic phases, respectively. In order to avoid local minima, calculation was carried out with the conjection direction method through refinement. The split pseudo-Voigt function was used for the profile function. Zr^4 , Y^3 and O^2 ions were used as chemical species. Through the refinement, occupancy of atom was fixed to $(Y_2O_3)_{0.03}(ZrO_2)_{0.97}$ in all phases. In the case of monoclinic phase, the linear constrain condition was applied for Zr and Y with respect to atomic positions. The linear constrain conditions for isotropic displacement parameters were also applied for Zr and Y in all phases. For the degradation samples, the prefered orientation (102) was used for monoclinic phase [15].

Results and discussion

The x ray diffraction data of the sintered body were analyzed by the Rietveld method. According to Ohmichi et al. [16], the cubic phase in 3Y TZP was detected as a function of sintering temperatures. Thus, the cubic and tetragonal models were first examined for the data from the samples sintered at 1500 . The reliability factors the weighted profile, Bragg intensity, and goodness of fit indicator were R_{wp} 6.66 , R_I 1.92 for the cubic phase, R_I 2.22 for the tetragonal phase, S 1.61. A small discrepancy attributable to the cubic structure was observed around the $(400)_{cubic}$ reflection. Recent studies on Y TZP showed the existence of a tetragonal phase with c/a 1 (so called pseudo cubic structure) [17, 18]. Thus, we made the refinement using the two tetragonal (named t1, t2) model.

Fig. 1 illustrates the profile fit and difference patterns of the revised Rietveld analysis of the sample sintered at 1500 . The region of $(400)_{tetra}$, $(004)_{tetra}$ reflections is enlarged as an inset. The two tetragonal model gave much less reliable factor than the cubic and tetragonal model. The reliable factors are R_{wp} 6.25, R_I 1.89 for t1 phase, R_I 1.78 for t2 phase, S 1.51. As the two tetragonal model gave much less reliable factors than the tetragonal and cubic model, we made the refinement for all samples using the two tetragonal model.

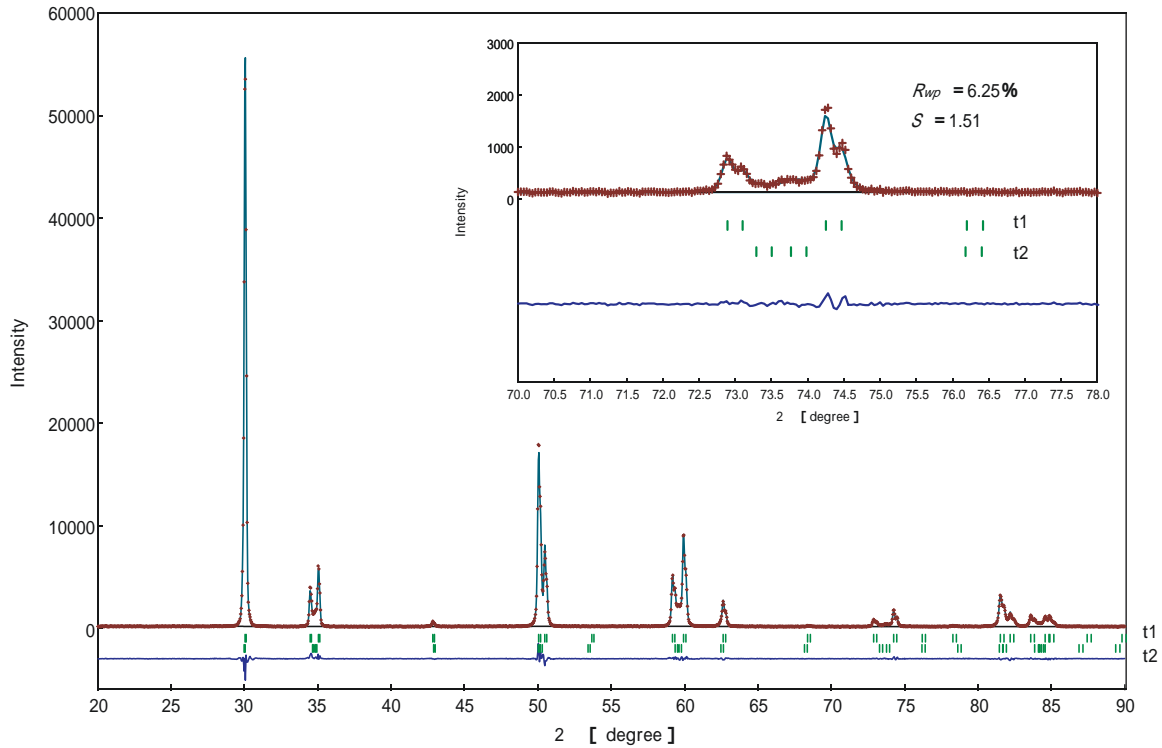The results obtained by the Rietveld analysis based on the two-tetragonal phase model (t1, t2) and the bulk

Fig.　Results of x-ray diffractometry and revised Rietveld analysis of the sample sintered at 1500℃. Dotted line: data obtained. Solid ilne: calculated intensity. Bars: angular position of possible Bragg reflection of t1, t2 phase. Plots at bottom: ($I_{calc}-I_{obs}$) difference. The region of $(400)_{tetra}$, $(004)_{tetra}$ reflections is enlarged as an inset.

Table　Bulk densities and results of Rietveld analysis of 3Y-TZP ceramics with two-tetragonal model ($P4_2/nmc$).

Sintering temp.(℃)	Density (g/cm³)	Phase	wt	Y₂O₃* (mol)	a (nm)	c (nm)	Atomic coordinates z	100 $U_{Zr,Y}$ (nm²)	100 U_O (nm²)	c_f/a_f	total Y₂O₃** (mol)	R_I ()	R_{wp} ()	S
1500	6.07	t1	76.3	2.46	0.36046(1)	0.51791(2)	0.209(1)	0.0004(8)	0.005(1)	1.0160	3.48	1.80	6.25	1.51
		t2	23.7	6.77	0.36248(5)	0.51550(1)	0.214(5)	0.014(4)	0.044(6)	1.0056		1.79		
1400	6.06	t1	85.4	2.75	0.36082(3)	0.51805(4)	0.211(1)	0.0017(9)	0.002(2)	1.0153	3.34	1.67	6.98	1.77
		t2	14.6	6.80	0.36236(6)	0.51530(1)	0.200(5)	0.013(6)	0.004(9)	1.0055		1.62		
1300	5.38	t1	92.1	3.02	0.36080(3)	0.51769(5)	0.212(1)	0.0033(8)	0.004(1)	1.0146	3.31	1.25	7.12	1.67
		t2	7.9	6.67	0.3621(1)	0.5151(2)	0.20(1)	0.002(8)	0.01(fixed)	1.0058		1.30		
1200	4.20	t1	90.8	3.17	0.36083(4)	0.51754(6)	0.210(1)	0.0007(8)	0.001(1)	1.0142	3.49	1.52	6.33	1.59
		t2	9.2	6.67	0.3621(1)	0.5151(3)	0.22(2)	0.017(9)	0.01(fixed)	1.0058		1.36		
1000	3.38	t1	91.2	3.21	0.36074(4)	0.51735(7)	0.212(2)	0.0025(9)	0.006(1)	1.0141	3.52	1.09	6.37	1.63
		t2	8.8	6.67	0.3621(1)	0.5151(3)	0.21(2)	0.02(1)	0.01(fixed)	1.0058		0.96		

*:calculated from eq.1 (see text).
**:calculated from eq.1 and fraction of t1, t2 phase.

densities of the sintered body are shown in Table 1. The fractional atomic coordinates of oxygen z and isotropic displacement parameters U are also given, where the thermal displacement parameter of oxygen is fixed in t2 phase for the samples sintered at 1100, 1200 and 1300℃. The Y₂O₃ concentration of each tetragonal phase was calculated from tetragonality (c_f/a_f) using the following equation [18], where a_f and c_f are the lattice parameters of a fluorite type structure ($a_f=\sqrt{2}a$, $c_f=c$).

$$\text{YO}_{1.5}\,\text{mol} = \frac{1.0223 - \frac{c_f}{a_f}}{0.001319} \qquad \cdots\cdots 1$$

The total Y₂O₃ concentration was calculated from Y₂O₃ concentration and weight fraction of each phase. The value of total Y₂O₃ concentration was slightly larger than that of the ideal one (3 mol). As the equation 1 was derived using the data of a metastable tetragonal phase (so called t' phase) that transformed from the high temperature cubic phase [19], a small discrepancy may be observed.

The tetragonality of t1 phase increased with the increase of sintering temperatures, while the tetragonality of t2 phase slightly decreased. The Y₂O₃ concentrations of t1 and t2 phases are plotted as a
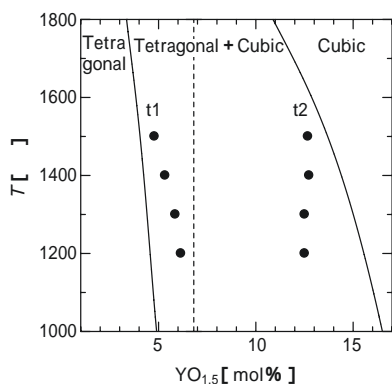
Fig.   Phase separation diagram of 3Y TZP ceramics. Solid circles correspond to $YO_{1.5}$ concentration of t1 (low yttrium) and t2 (high yttrium) phases. Solid line refers to equilibrium phase boundary proposed by Scott[20]. Broken line referes to yttrium concentration of starting powder.
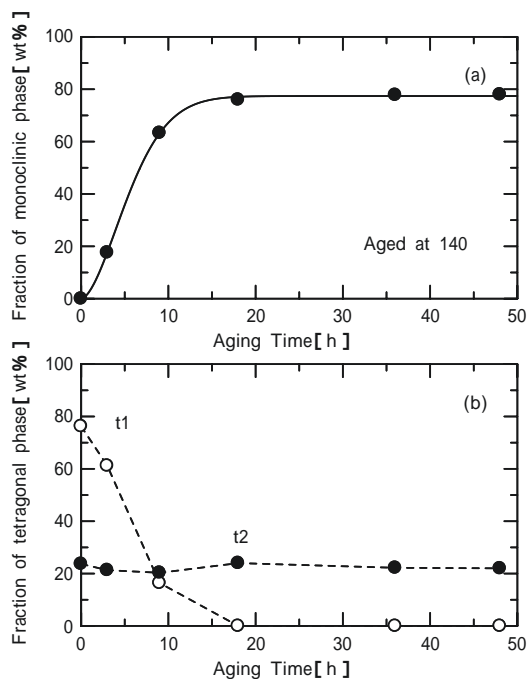

Fig.   Kinetics of tetragonal to monoclinic phase transition of the sample sintered at 1500 under hydrothermal conditions. Aging time dependence of fraction is plotted for monoclinic phase in (a) and for tetragonal phases in (b). Solid line corresponds to a curve fitted using the Johnson Mehl Avrami equation (see text).

function of sintering temperature in Fig.2, where the phase diagram proposed by Scott [20] is also given (Note that the phase boundary is shifted by 0.5 mol Y_2O_3 due to the discrepancy mentioned above.).

As the crystal structure of the starting powder is tetragonal phase with a uniform 3 mol Y_2O_3 distribution, Fig.2 reflects the process of phase separation in the sintered body toward an equilibrium state. Phase separation is strongly promoted for the samples sintered at 1400 and 1500 . On the other hand, the sintering body is less separated at lower temperatures. According to the phase diagram, the sintered body should be separated into the tetragonal and cubic phase in an equilibrium state. However, when equilibrium is not reached under the sintering conditions, the structure of the sintered body is frozen in a nonequilibrium state. As a result, two tetragonal regions of low (t1 phase with c/a 1) and high yttrium (t2 phase with c/a 1) concentrations are formed. It is note worthy that the structure is assigned to the tetragonal phase of c/a 1 even in the high yttrium region. Although a simple cubic phase has been considered for the high yttrium region in 3Y TZP ceramics, the nonequilibrium tetragonal phase is more plausible in the case of usual sintering conditions.

Recent studies using high resolution TEM[8 10] revealed that enrichment of yttrium exclusively occurs along the grain boundary (so called segregation), and continuous distribution of yttrium was reported on 3Y TZP. Although simple two tetragonal model was used

for the Rietveld analysis, such microscopic heterogeneity should be considered in further analysis.

Hydrothermal degradation experiments were performed on the sample sintered at 1500 and the results are shown in Fig.3. The fractions of t1, t2 and monoclinic phases induced by hydrothermal degradation are plotted as a function of aging time. At early stage of degradation, the monoclinic phase increases with increasing aging time, while the low yttrium region (t1 phase) decreases. The t1 phase is completely transformed into monoclinic phase during degradation. On the other hand, the t2 phase is stable even after long time aging. It is clear that the tetragonal phase of low yttrium concentration is exclusively transformed into monoclinic phase under the hydrothermal conditions.

Yasuda *et al.* [21] obserevd a heterogeneous structure attributed to the high and low yttrium concentration regions in 3Y TZP ceramics, and the low yttrium region is selectively transformed into monoclinic phase at early stage of hydrothermal degradation. Ohmichi *et al.* [19] also revealed the formation of tetragonal phase of low Y_2O_3 concentration. They reported that the

reduction of yttrium concentration in tetragonal phase promotes the degradation of sintered body. In order to clarify the correlation between the phase separated structure and hydrothermal degradation mechanism, further consideration was made on the kinetics of the tetragonal to monoclinic phase transition.

It is known that the kinetics of tetragonal to monoclinic phase transition is given by the Johnson Mehl Avrami equation[22]. Thus, the time dependence of monoclinic fraction is analyzed using the following general equation.

$$f_m = b(1 - \exp(-at^n)) \qquad \cdots\cdots 2$$

where f_m is fraction of monoclinic phase, t is aging time and n is the dimension of growth of nucleation. Parameter a is rate constant for phase transition. Parameter b is a value of the fraction when the phase transition is complete under the hydrothermal conditions. These parameters are determined by the nonlinear least square fitting method.

The values of parameters are $a = 0.0397\,h^{-1}$, $b = 77.4$, $n = 1.70$. The calculated results are shown by a solid line in Fig. 3. If the transition preceeds via homogeneous nucleation and growth mechanism, the value of parameter n should be 3～4. However, the value of parameter n is determined as $n = 1.70$. This suggests operation of highly heterogeneous nucleation and growth mechanism in the tetragonal to monoclinic phase transition. Parameter a implies a rate of transition. It has been considered that the stability of tetragonal phase is influenced by crystal size (grain size)[2] and concentration of yttrium[23]. Therefore, the parameter a is governed by the concentration of yttrium in transformable phase as well as grain size. Parameter b indicates a fraction of transformable tetragonal phase. The value of transformable tetragonal phase is determined as $b = 77.4$. This value is in good agreement with the result from Rietveld analysis (fraction of t1 phase: 76.3).

It is known that 3Y TZP does not transform into monoclinic phase completely under hydrothermal conditions[16,23]. Such saturation behavior has been explained in terms of grain size, anisotropic coefficient of expansion, and compressive stress due to the transformation[23]. However, the Rietveld analysis clearly shows that the untransformable region of 3Y

TZP ceramics is attributable to the formation of high yttrium region. Under hydrothermal conditions, the low yttrium region can be easily transformed into monoclinic phase, while the high yttrium region remains unchanged because of its resistance to transform. Hydrothermally transformable fraction in 3Y TZP ceramics is governed by the amount of low yttrium region. Thus, we may conclude that the formation of the low yttrium region due to phase separation is responsible for the hydrothermal degradation of 3Y TZP ceramics.

Conclusion

The crystal structure of 3Y TZP ceramics has been studied using x-ray diffractometry. The sintered body underwent phase separation into high and low yttrium regions with the increase of sintering temperature. Tetragonal phase was assigned both regions. The high yttrium region was analyzed using a tetragonal phase model with $c/a = 1$. The amount of monoclinic phase induced by hydrothermal degradation increased with increasing degradation time, while that of the low yttrium region decreased. The fraction of transformable phase evaluated by the Johnson Mehl Avrami equation was in good agreement with the fraction of t1 phase (low yttrium region) determined by the Rietveld analysis. Quantitative analyses clearly showed that the low yttrium region selectively transforms into monoclinic phase under hydrothermal conditions, while the high yttrium region remains unchanged. Hydrothermally transformable fraction in 3Y TZP ceramics is governed by the amount of low yttrium region. Thus, the formation of low yttrium region due to phase separation is responsible for the hydrothermal degradation of 3Y TZP ceramics.

Reference

K. Tsukuma, K. Ueda, and M. Shimada, *J. Am. Ceram. Soc.,* 68 (1), C4 C5 (1985).

F. F. Lange, *J. Mater. Sci.,* 17 (1), 225 63 (1982).

F. F. Lange, G. L. Dunlop, and B. I. Davis, *J. Am. Ceram. Soc.,* 69 (3), 237 40 (1986).

F. Y. Ho, and W. C. Wei, *J. Am. Ceram. Soc.,* 82 (6), 1614 16 (1999).

T. Sato, and M. Shimada, *J. Am. Ceram. Soc.,* 68 (6), 356 59 (1985).

M. Yoshimura, T. Noma, K. Kawabata, and S. Somiya, *J. Mater. Sci. Lett.,* 6 (4), 465 67 (1987).

S. Stemmer, J. Vleugels, and O. Van Der Biest, *J. Eur. Ceram. Soc.,* 18 (11), 1565 70 (1998).

K. Matsui, H. Horikoshi, N. Ohmichi, M. Ohgai, H. Yoshida, and Y. Ikuhara, Y., *J. Am. Ceram. Soc.,* 86 (8), 1401 8 (2003).

K. Matsui, N. Ohmichi, M. Ohgai, H. Yoshida, and Y. Ikuhara, *J. Ceram. Soc.Jpn,* 114 (3) 230 37 2006

10 K. Matsui, N. Ohmichi, M. Ohgai, H. Yoshida, and Y. Ikuhara, *J. Mater. Res.,* 21 (9) 2278 2289 (2006)

11 F. Izumi, and T. Ikeda, *Mater. Sci. Forum,* 321 324, 198 203 (2000).

12 M. Yashima, S. Sasaki, M. Kakihana, Y. Yamaguchi, H. Arashi, and M. Yoshimura, *Acta. Cryst.,* B 50, 663 72 (1994).

13 M. Morinaga, J. B. Cohen, and J. Faber Jr, *Acta Cryst.,* A 35, 789 95 (1979).

14 C. J. Howard, R. J. Hill, and B. E. Riechet, *Acta Cryst.,* B 44, 116 20 (1988).

15 N. Hiramatsu, and H. Maruyama, Preferred Orientation Texture in Transformed Zirconia ; pp 119 32 in *Zirconia Ceramics Vol 13, 14* Edited by S. Nishida, T. Masagi and S. Somiya. Uchida Rokakuho Publishing Co., Tokyo, 1984 [in Japanese].

16 N. Ohmichi, K. Kamioka, K. Ueda, K. Matsui, and M. Ogai, *J. Ceram. Soc. Jpn.,* 107 (2) 128 33 (1999) [in Japanese].

17 F. Sanchez Bajo, I. Cachadina, J. D. Solier, F. Guiberteau, and F. L. Cumbrera, *J. Am. Ceram. Soc.,* 80 (1), 232 36 (1997).

18 I. R. Gibson, and J. T. S. Irvine, *J. Am. Ceram. Soc.,* 84 (3), 615 18 (2001).

19 R. A. Miller, J. L. Smialek, and R. G. Garlick, Phase Stability in Plasma Sprayed, Partially Stabilized Zirconia Yttria ; pp. 241 55 in Advances in Ceramics, Vol. 3, *Science and Technology of Zirconia.* Edited by A. H. Heuer and L. W. Hobbs. American Ceramics Society, Columbus, OH, 1981.

20 H. G. Scott, *J. Mater. Sci.,* 10 (9), 1527 35 (1975).

21 K. Yasuda, S. Arai, M. Itoh, and K. Wada, *J. Mater. Sci.,* 34 (15), 3597 3604 (1999).

22 M. Avrami, *J. Chem. Phys.,* 7, 1103 (1939).

23 M. Yashima, T. Nagatone, T. Noma, N. Ishizawa, Y. Suzuki, and M. Yoshimura, *J. Am. Ceram. Soc.,* 78 (8), 2229 32 (1995).

Isao YAMASHITA   Koji TSUKUMA
     15 4   1   50 4   1